

NJC

Accepted Manuscript



This is an *Accepted Manuscript*, which has been through the Royal Society of Chemistry peer review process and has been accepted for publication.

Accepted Manuscripts are published online shortly after acceptance, before technical editing, formatting and proof reading. Using this free service, authors can make their results available to the community, in citable form, before we publish the edited article. We will replace this *Accepted Manuscript* with the edited and formatted *Advance Article* as soon as it is available.

You can find more information about *Accepted Manuscripts* in the [Information for Authors](#).

Please note that technical editing may introduce minor changes to the text and/or graphics, which may alter content. The journal's standard [Terms & Conditions](#) and the [Ethical guidelines](#) still apply. In no event shall the Royal Society of Chemistry be held responsible for any errors or omissions in this *Accepted Manuscript* or any consequences arising from the use of any information it contains.

Hexagonal Columnar Liquid Crystal as a Processing Additive to P3HT: PCBM Photoactive Layer

Ahipa T.N., Anoop K.M. and Ranjith Krishna Pai *

Nanostructured Hybrid Functional Materials and Devices, Center for Nano and Material
Sciences, Jain University, Jain Global Campus, Bangalore – 562112, India

* E-mail: ranjith.pai@jainuniversity.ac.in

Abstract

Morphology of the donor/acceptor network in the photoactive layer is critical in order to optimize the device performance. In the present study, new trihydrazone-functionalized cyanopyridine (CPTH-D16) demonstrating ambient temperature hexagonal columnar liquid crystalline phase is introduced into the well-known photoactive layer *i.e.* P3HT:PCBM as processing additive towards the construction of an efficient solar cell. Photon absorption and emission properties of the blends in solution/film state are systematically investigated by UV-visible and fluorescence spectroscopy. Further, surface morphology, degree of crystallinity, changes in nanostructure, and conductivity of the blend films are observed through epi-fluorescence and atomic force microscopy. It is observed that the addition of CPTH-D16 liquid crystal drastically increases the TUNA current passing throughout the P3HT:PCBM film. Here, the structural anisotropic nature of CPTH-D16 material helps to obtain well-ordered morphology with nanostructured crystallite formation as well as the enhanced current in the P3HT:PCBM film.

Keywords: polymer solar cell, optical property, epi-fluorescence microscopy, liquid crystal, atomic force microscopy.

1. Introduction

Nowadays, solution-processed organic solar cells (OSCs) are under immense investigation due to their advantages of low cost, lightweight and flexibility in large area applications.^[1, 2] Currently, the performance of OSCs has increased dramatically and power conversion efficiency up to 9% has been obtained by exploiting low band-gap polymers.^[3] Record-breaking power conversion efficiency (PCE) up to 10.6% was also attained in the tandem polymer solar cells.^[4] To improve the PCE, various studies have been carried out including the design and synthesis of new low band gap polymers,^[5, 6] improving the understanding of bulk heterojunction (BHJ) device physics^[7] and developing the novel device fabrication methods and structures.^[8-10]

Among the different organic photovoltaic devices, the study of BHJ solar cell devices is one of the foci of today's research interest. In general, BHJ solar cell devices are constructed by sandwiching the blend (made up of electron donating p-type conjugated polymers and electron-accepting n-type fullerene derivatives) between the anode and cathode. In order to get improved PCE of BHJ solar cells, uninterrupted pathways must be formed to allow the excited electrons and created holes to transfer to the external circuit without recombining with each other. The well-known BHJ solar cell comprised of poly (3-hexylthiophene-2,5-diyl) (P3HT) as an electron donor and [6,6]-phenyl-C61-butyric acid methyl ester (PCBM) as an electron acceptor exhibited a quite promising PCE. However, inherent space charge effects and the unfavorable morphology in the BHJ structure are the major drawbacks for achieving high PCE. In addition, obtaining an ordered bicontinuity of the microphase, which ensures optimum charge-carrier photogeneration, extraction and transfer to the electrodes are the most critical challenges in organic polymer solar cells.^[11-13] To avoid these challenges, various approaches such as thermal annealing, post-fabrication annealing at high temperature, and additives have been successfully demonstrated in the literature to develop an optimum morphology with

minimum phase separation as well as the formation of nano-crystalline domains in the blends to achieve the improved PCE.^[14-19]

From the past few years, liquid crystalline materials have been studied extensively because of their unique electronic and optoelectronic properties.^[20-29] Among the various liquid crystal phases, materials exhibiting columnar phase have been utilized systematically as promising organic semiconductor candidates in the area of optoelectronic devices because of their highly ordered structures and corresponding high charge-transport mobilities.^[30] In general, highly ordered LC materials possess the high degree of anisotropy and can be easily controlled by simple thermal annealing. Also, the LC materials have the tendency to form an anisotropic film even mixed with P3HT:PCBM. Therefore, the addition of LC facilitates for the fabrication of an efficient photovoltaic device.

Recently, Chen and co-workers have exploited the potential applications of poly-3-hexylthiophene (P3HT) based liquid crystalline rod-coil block copolymers in polymer solar cells.^[31] They prepared two new liquid crystalline copolymers carrying a rod-like liquid crystal block poly(4-(dodecyloxy)-4''-(oct-7-en-1-yloxy)-1,1',4',1''-terphenyl), and a discotic liquid crystal block poly(2,3,6,7,10-pentakis(hexyloxy)-11-(oct-7-en-1-yloxy)triphenylene), respectively. According to authors, the thermal treatment of liquid crystalline block copolymers blended with PCBM exhibit the power conversion efficiency up to 4.03% with the improved photovoltaic performance. The improved performance is due to the efficient exciton separation of the active layer caused by the self-assembling nature of liquid crystalline block at the donor and acceptor interface which results in enhanced crystallization and ordering of P3HT chains as well as for the formation of interpenetrating networks. Further, they demonstrated that the copolymer with the discotic liquid crystal block is more favorable than the one with rod-like liquid crystal block, because of the greater compatibility with the fullerene acceptors and the more efficient charge transport caused by the self-assembled columnar phase from the discotic

liquid crystals. Against this background, the addition of columnar liquid crystal material into the P3HT:PCBM system as processing additive helps to achieve the optimized morphology and to promote the high charge mobility in it.

In the present work, trihydrazone functionalized cyanopyridine (CPTH-D16) liquid crystal material capable of exhibiting ambient temperature hexagonal columnar phase is introduced into the P3HT:PCBM system with the goal of developing nanostructured crystallite and an improved bicontinuous phase separation in the prepared film with enhanced photophysical and conducting properties, which are the essential criteria's for the construction of high efficient solar cells. Further, UV-visible absorption, fluorescence emission, surface morphology and conductive properties of the newly designed P3HT:CPTH-D16:PCBM (1:0.5:0.5) blend film was investigated using spectrophotometer, epi-fluorescence and atomic force microscopic techniques.

2. Material and Methods

Regioregular electronic grade P3HT polymer with an average Mn of 15,000-45000 and a fullerene derivative (PCBM) were purchased from Sigma-Aldrich source and used without further purification. Trihydrazone-functionalized cyanopyridine (CPTH-D16) was prepared by using our already reported procedure and used as a liquid crystalline additive.^[32] This additive is capable of exhibiting hexagonal columnar phase over a wide temperature range (from ambient to 81.3 °C). The spectrophotometric grade chloroform solvent was purchased from Merck and was used as received.

The desired material/ blend solutions of CPTH-D16, P3HT:PCBM (1:0.5 w/w), P3HT:CPTH-D16 (1:0.5 w/w), CPTH-D16:PCBM (0.5:0.5 w/w), P3HT:CPTH-D16:PCBM (1:0.5:0.5 w/w) were prepared from spectrophotometric grade chloroform solvent. Their photon absorption and emission properties were measured using UV-1800 SHIMADZU UV-

spectrophotometer and RF-5301 PC, SHIMADZU spectrophotometer equipped with a Xe-lamp as an excitation source. Further, the thin films of material/ blend solution were prepared by drop casting over the pre-cleaned transparent conducting ITO substrate and their uniform films were obtained after annealing the films at 80 °C for specified interval of time (i.e. 5 minutes). The surface morphology of the prepared films were later investigated by epifluorescence (Moticam Pro 205 A) and AFM (Bruker Dimension Icon) microscopes. Also, their conductivity measurements were carried out using PeakForce-TUNA™ techniques.

3. Results and discussion

The chemical structure of P3HT, PCBM and CPTH-D16 is shown in **Figure 1**. CPTH-D16 exhibiting ambient temperature hexagonal columnar phase was synthesized as per our earlier report.^[32] UV-visible absorption properties of material/ blend in chloroform solution were recorded and their spectrum is shown in **Figure 2**. A strong absorption band was observed at 320 nm for CPTH-D16 solution, which is attributed to π - π^* electronic transition occurring in the molecule. However, an equivalent addition of CPTH-D16 to PCBM solution showed a slightly bathochromic shift in absorption band (~ 6 nm) when compared to the absorption band of CPTH-D16 alone. In fact, in solution state, PCBM material is also exhibit an absorption band in the range of 325-335 nm. Thus, the observed single absorption band at 326 nm can be assigned to the cumulative effect of CPTH-D16 and PCBM materials. On the other hand, the addition of CPTH-D16 to P3HT solution (1:0.5 ratio) showed two absorption bands, one at 332 nm (higher energy band) and another at 453 nm (lower energy band), respectively. Here, the lower energy band is mainly due the π - π^* transition occurring in the P3HT polymer. Similarly, the ternary solution of P3HT:CPTH-D16:PCBM (1:0.5:0.5 ratio) also showed two absorption bands with decreased intensity in the higher energy absorption band. But, in absence of CPTH-D16, a significantly decreased band intensity in the higher energy band was observed without affecting the intensity of lower energy band in P3HT:PCBM solution (1:0.5 ratio).

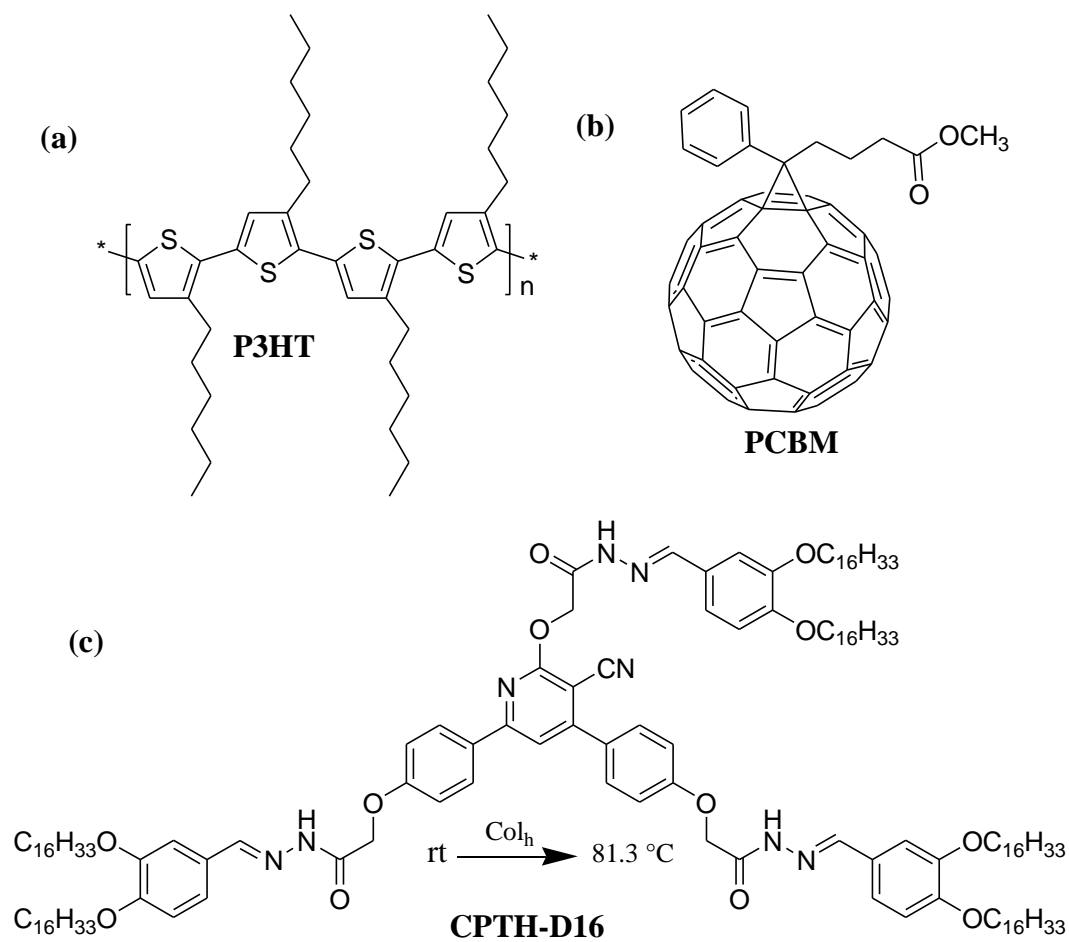


Figure 1. The chemical structure of (a) P3HT; (b) PCBM; (c) CPTH-D16 with temperature range of hexagonal columnar (Col_h) phase.

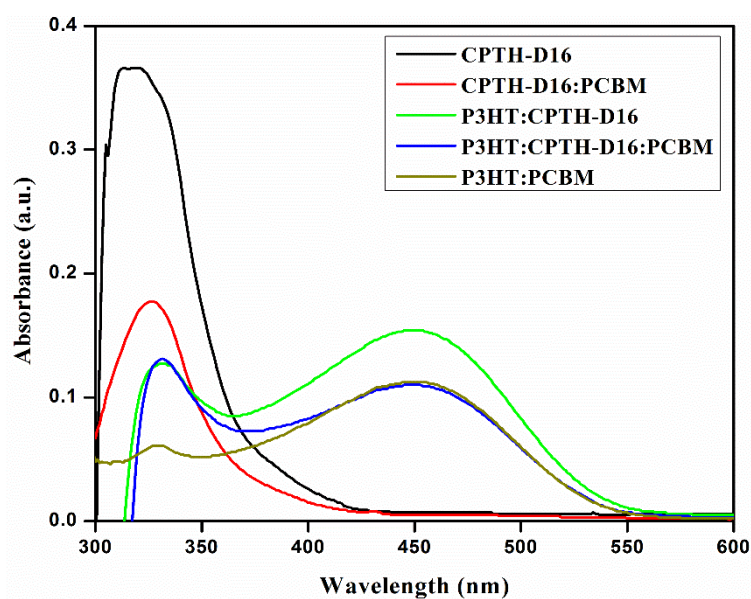


Figure 2. UV-visible absorption spectra of material/ blend solutions.

In order to determine the charge transfer process between the donor P3HT and the acceptor PCBM in the solution state, further, fluorescence emission properties of P3HT:CPTH-D16, P3HT:CPTH-D16:PCBM and P3HT:PCBM blend solutions were examined under the excitation wavelength of 450 nm and their spectra is shown in **Figure 3**. In all the cases, an emission band was observed at 568 nm. The fluorescence signal from P3HT:PCBM was fairly quenched by adding CPTH-D16 into the blend solution, indicates that an improved photo induced charge transfer occurring between the P3HT and PCBM.^[33-36] Thus, the liquid crystalline CPTH-D16 additive seems to either assist the formation of ordered P3HT phase, facilitating exciton/charge migration or increases the interfacial area between P3HT and PCBM for exciton dissociation by reducing the aggregation of P3HT.

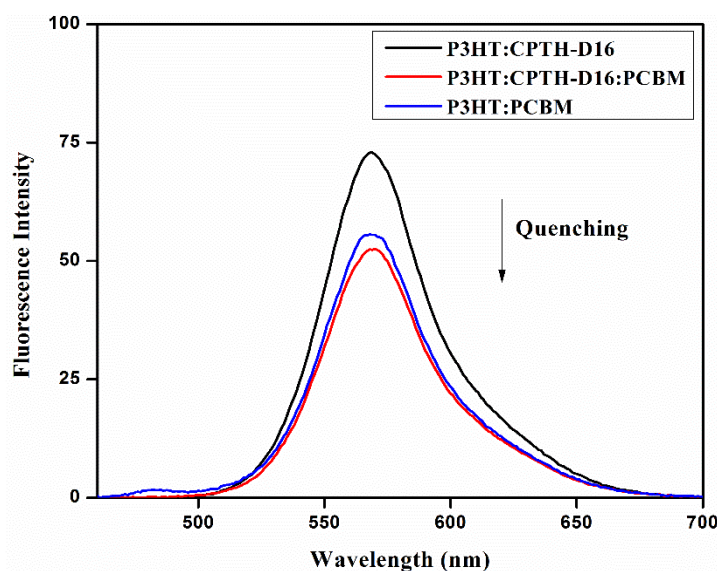


Figure 3. Fluorescence emission spectra of blend solutions

More often, solar cell device performance is mainly affected by the carrier mobility of the photoactive film. This can be effectively overcome by obtaining the well aligned polymer chains in the film. In fact, macroscopically ordered organic conducting polymers (due to π - π overlap between successive layers) possess an anisotropic structure as well as high conductivity along the chain direction. In general, the maximum absorption wavelength of the polymer (P3HT) in the film state is bathochromically shifted when compared to the solution spectra,

which is due to the major conformational order, resulting in different energy levels distribution.^[37] Consequently, the study of absorption behavior in thin film state is one of the essential criteria to determine the suitability of the blend material for the construction of high efficient solar devices. Films of P3HT:CPTH-D16:PCBM and P3HT:PCBM were prepared over the cover slip and annealed at 80 °C for 5 minutes. Their absorption spectra is depicted in **Figure 4**. The absorption spectrum of P3HT:PCBM blend film exhibit the characteristic vibronic peaks at 510, 550 and 603 nm in the visible range is an indication of crystallinity of the P3HT domains.^[38, 39] In particularly, an absorbance at 510 nm is assigned to the inter-chain delocalized excitation and an absorbance at 550 nm is attributed to the local order of P3HT as well as a peak at 603 nm is ascribed to the better crystallinity of P3HT.^[38] Further, an additional less intensity peak at 330 nm is due to the absorbance of PCBM material. However, in case of ternary P3HT:CPTH-D16:PCBM blend film, the visible absorption band intensities are slightly decreased compared to the binary blend film. But, a drastically increased intensity band at 330 nm in the ultraviolet region is observed. This absorption band is originate from the electronic transitions of CPTH-D16:PCBM materials. Apart from the absorption in the ultraviolet and visible region, the ternary film exhibits an improved absorption in the NIR region (700-900 nm). Thus, it is important to note that the added liquid crystalline CPTH-D16 material into the P3HT:PCBM layer causes the major conformational order resulting in different energy levels distribution, which further significantly contribute to achieve a wide absorption property in the film.

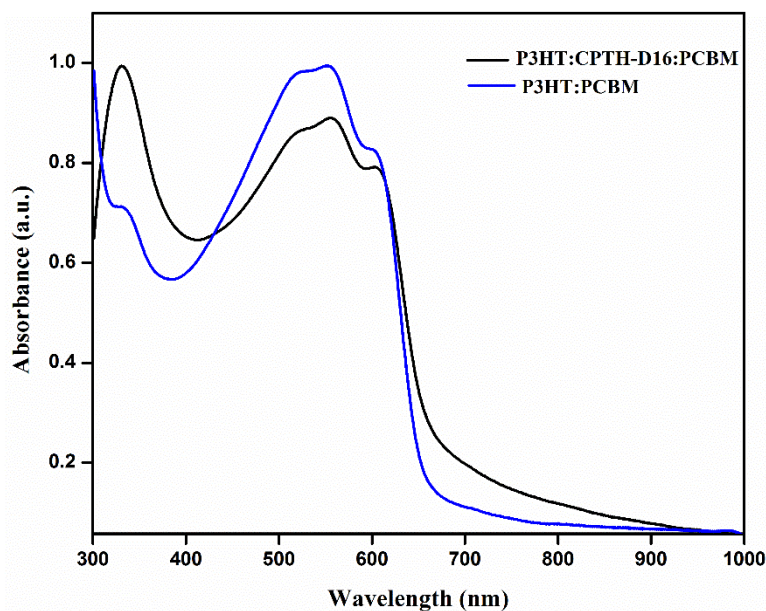


Figure 4. UV-visible absorption spectra of P3HT:CPTH-D16:PCBM and P3HT:PCBM in film state.

It is well established that the dispersed heterojunction films of donor-acceptor organic materials have high quantum efficiencies compared to the planar hetero-junction films. This is mainly because; an exciton formed in the dispersed heterojunction film can more easily find an interface within its diffusion length. In addition to this, the desired film morphology has a drastic effect on achieving the high quantum efficiency. Generally, the presence of voids and rough surfaces in the films are the prime factors lead to the chance of short-circuit and increase of series resistance. In order to overcome these drawbacks, the formation of phase-separated interpenetrating donor-acceptor interface inside the thin film is found to be one of the essential requirement to obtain better device performance.^[40]

In most of the P3HT:PCBM blend compositions, phase separation and nanoscale interpenetrating network formations takes place only after annealing the film at high temperature. This network is essential in polymer solar cells, wherein the nanoscale interpenetrating networks provide both efficient charge separation and charge collection at the electrodes.^[41] To determine interpenetrating network in the present work, epi-fluorescence

microscopic images were recorded under UV light for P3HT:PCBM; CPTH-D16; P3HT:CPTH-D16; CPTH-D16:PCBM and P3HT:CPTH-D16:PCBM films respectively. Their epi-fluorescence images are shown in **Figure 5 (a-e)**. The less interpenetrating network was noticed for the P3HT:PCBM film in **Figure 5 (a)**, whereas, the crystalline nature was seen in the film of liquid crystal material *i.e.* CPTH-D16, as shown in **Figure 5 (b)**. Generally, the conformation and degree of order of the P3HT polymer chains in the active layer plays a crucial role in effective charge separation and transport process.^[42, 43] Further, the addition of columnar liquid crystalline CPTH-D16 induce the crystallinity of P3HT, and co-crystallize with P3HT chains, resulting in a long range crystallinity of P3HT domains and favorable interpenetrating networks (**Figure 5 (c)**). Similar kind of interpenetrating network and nanocrystallite formation was observed in CPTH-D16:PCBM film (**Figure 5 (d)**). However, it is interesting to note that, in case of ternary P3HT:CPTH-D16:PCBM film an enhanced interpenetrating network was perceived, wherein, the brighter region is made up of P3HT polymer and darker region is of PCBM material. Further, these two layers are sandwiched by CPTH-D16 additive.

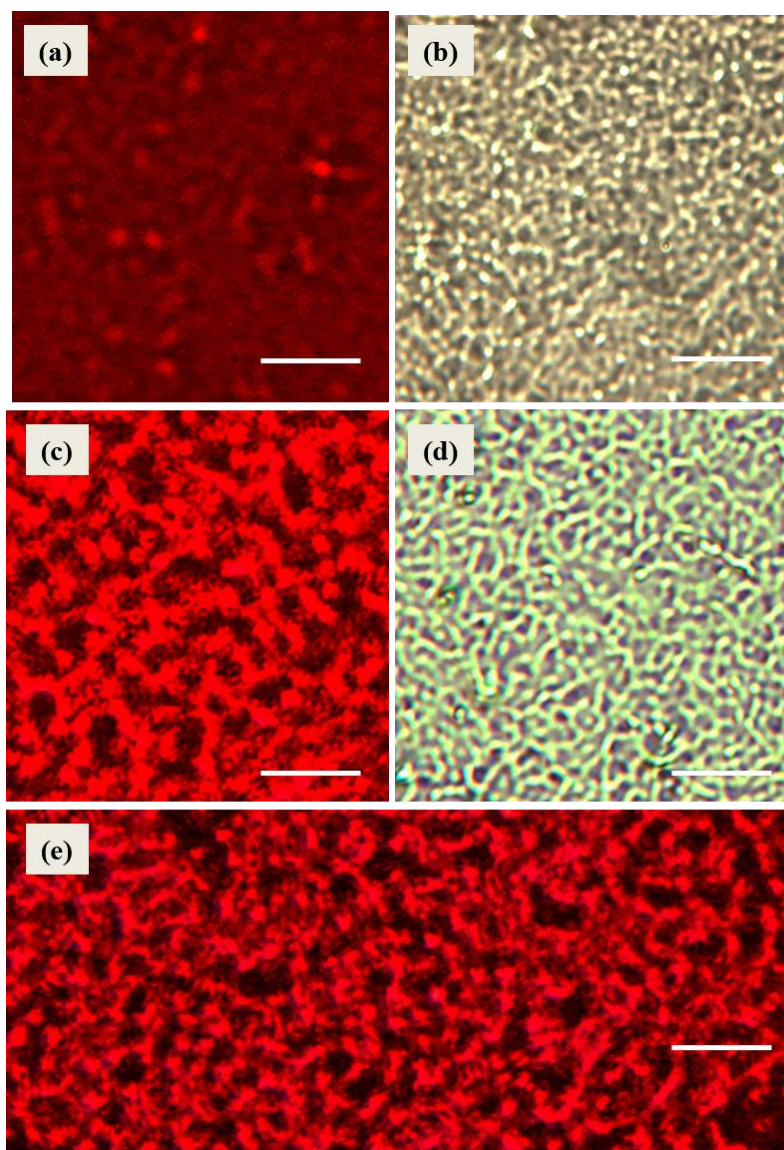


Figure 5. Epi-fluorescence microscopic (scale bar: 100 μm) images under UV light (a) P3HT:PCBM (1:0.5) film (b) CPTH-D16 film (c) P3HT:CPTH-D16 (1:0.5) film (d) CPTH-D16:PCBM (0.5:0.5) film (e) P3HT:CPTH-D16:CPTH-D16 (1:0.5:0.5) film, respectively.

In fact, controlling the domain size of the donor and acceptor interpenetrating networks is essential for optimizing BHJ device performance. It is important to note that, the charge generation process is less efficient in case of large sized domains due to the small fraction of excitons reach the donor/acceptor interface. In ideal condition, the domain size should be similar to or slightly smaller than the exciton diffusion length. Typically, the exciton diffusion length in organic semiconductors as well as in conjugated polymers is approximately limited to 10 nm.^[44] However, the effect of liquid crystalline CPTH-D16 material on the thickness of

interpenetrating network were investigated in case of P3HT:CPTH-D16; CPTH-D16:PCBM; and P3HT:CPTH-D16:PCBM films by measuring the thickness of channel at four different places (*i.e.* A, B, C, and D), as shown in **Figure 6** and an average thickness of 66.83, 27.07 and 25.97 μm respectively were noticed. This clearly indicates that the P3HT:CPTH-D16:PCBM ternary film is made-up of well-defined bicontinuous microphase region without significant PCBM aggregation. Thus, the observed morphology and the interpenetrating networks may induce effective charge transfer in the ternary composition film.

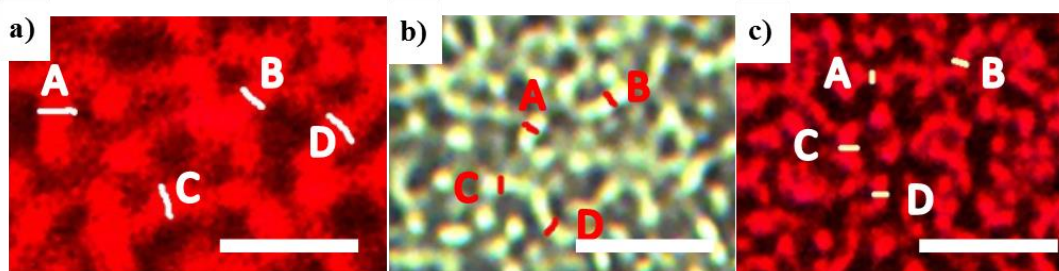


Figure 6. Measured area and thickness of interpenetrating network (scale bar: 100 μm) in the films of (a) P3HT:CPTH-D16; (b) CPTH-D16:PCBM; (c) P3HT:CPTH-D16:PCBM, respectively.

Figure 7 to 9 illustrates the morphologies and conductive properties of active layers (CPTH-D16, P3HT:CPTH-D16; CPTH-D16:PCBM and P3HT:CPTH-D16:PCBM) under the optimized condition recorded by atomic force microscopy (AFM). The obtained root-mean-squared surface roughness (R_{max}) and corresponding vertical heights are summarized in **Table 1**.

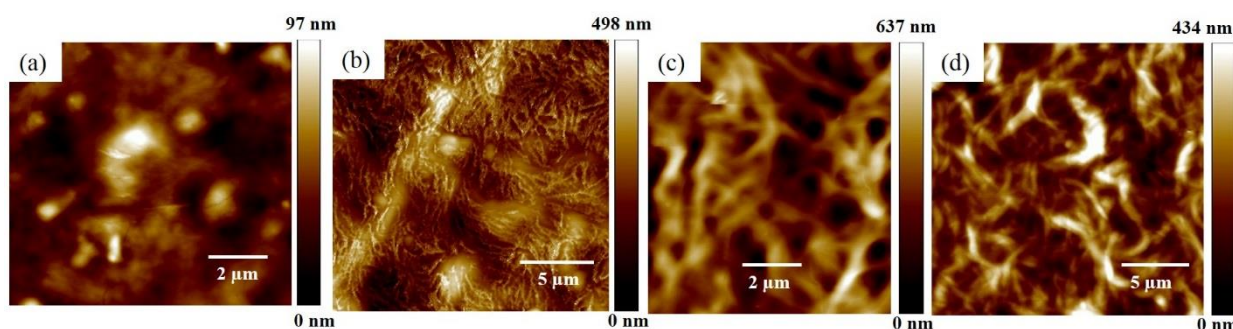


Figure 7. Topographical images of (a) CPTH-D16 film; (b) P3HT:CPTH-D16 film; (c) CPTH-D16:PCBM film; (d) P3HT:CPTH-D16:PCBM film, respectively.

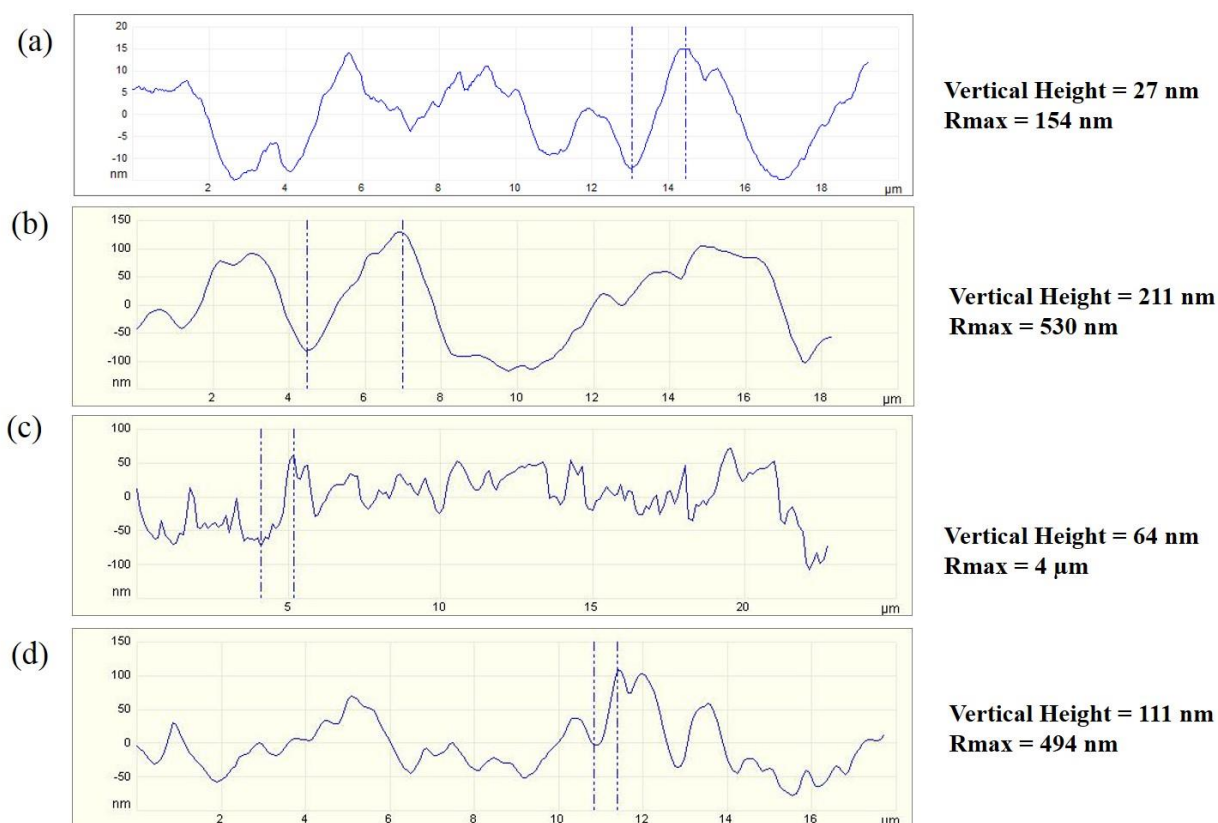


Figure 8. Vertical height profiles of (a) CPTH-D16 film; (b) P3HT:CPTH-D16 film; (c) CPTH-D16:PCBM film; (d) P3HT:CPTH-D16:PCBM film, respectively.

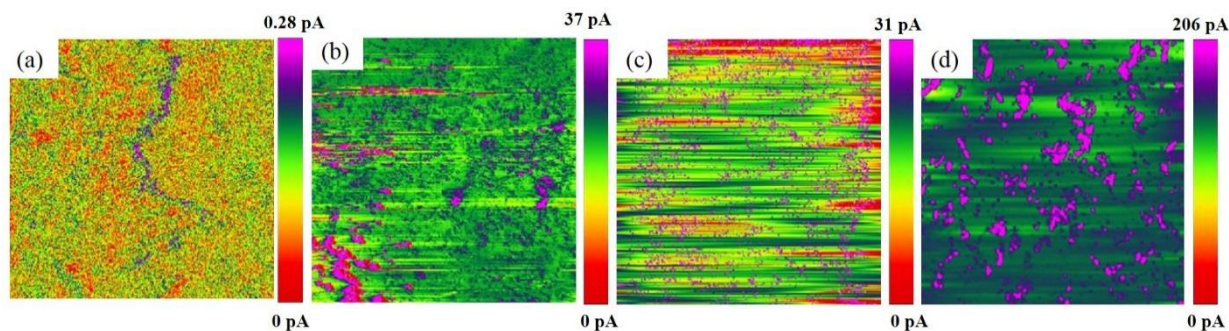


Figure 9. PeakForce-TUNA™ current (brighter colors are higher values) of (a) CPTH-D16 film; (b) P3HT:CPTH-D16 film; (c) CPTH-D16:PCBM film; (d) P3HT:CPTH-D16:PCBM film, respectively.

Table 1. Rmax, vertical height, current values for CPTH-D16:PCBM, P3HT:CPTH-D16, and P3HT:CPTH-D16:PCBM blend films.

	CPTH-D16	CPTH-D16:PCBM	P3HT:CPTH-D16	P3HT:CPTH-D16:PCBM
Rmax (nm)	154	4000	530	494

Vertical height (nm)	27	64	211	111
----------------------	----	----	-----	-----

For CPTH-D16 film, R_{\max} and vertical height are 154 nm and 27 nm, respectively. The addition of CPTH-D16 to P3HT layer results in the increased R_{\max} and vertical height of 530 nm and 211 nm. Similarly, the addition of CPTH-D16 to PCBM layer results in the increased R_{\max} and vertical height of 4 μm and 64 nm, respectively. Fascinatingly, the ternary P3HT:CPTH-D16:PCBM film exhibit R_{\max} and vertical height of 494 nm and 111 nm, respectively. Further, the observed roughness value for the ternary film is intermittent to that of the of P3HT:CPTH-D16 and CPTH-D16:PCBM films. This clearly confirms that the ternary film composed of the homogenized materials with nanocrystallite formation.

The PeakForce-TUNA™ conducting AFM measurements were further performed on the films in order to extract information on the nanoscale charge carrier transport. From **Figure 9**, it is evident that the mean current of 0.28 pA is observed for the liquid crystal CPTH-D16 film. It is important to note that, a fairly low and uniform current distribution on the order of 4 pA was observed for the P3HT films in the literature.^[45, 46] Interestingly, P3HT:CPTH-D16 (1:0.5 w/w) film prepared with the addition of CPTH-D16 to donor P3HT material exhibit the enhanced mean current of 37 pA. Similarly, CPTH-D16:PCBM (0.5:0.5 w/w) film also exhibit enhanced mean current of 31 pA. In both the cases, the addition of liquid crystal material drastically boosted the charge carrier ability of the donor and acceptor materials. Remarkably, the ternary film of P3HT:CPTH-D16:PCBM (1:0.5:0.5 w/w) show the significantly enhanced mean current of 206 pA. This high electrical conductivity is attributed to the improved nanocrystallization and orientation of P3HT in the film caused by the addition of columnar liquid crystalline CPTH-D16. Here, the observed mean current for ternary film is almost twenty times more when compared to mean current of 12.6 pA for the P3HT:PCBM (1:1 w/w) film, as

reported in the literature.^[19] In fact, the mean current is mainly depends on the geometry of the tip and the contact force between the tip and the sample. Thus, we utilized the same tip and the same contact force for all the conductive measurements to compare the current levels of different samples, at a given applied bias. Overall, the enhanced interpenetrating network, roughness and nanocrystallite of the ternary film are susceptible for the observed high conductivity. Thus, obtained high conductivity and superior interpenetrating network in the P3HT:CPTH-D16:PCBM film may effectively overwhelmed some of the prerequisite criteria's for the construction of high efficient photovoltaic cells.

4. Conclusion

In conclusion, the morphology of the donor/acceptor network in the photoactive layer is critical in order to optimize the device performance. In this work, we report a strategy for obtaining marked improvement in surface morphology and electrical conductivity of P3HT:PCBM photoactive layer by the addition of ambient temperature hexagonal columnar liquid crystalline material (CPTH-D16). In the ternary film, we observed an excellent interpenetrating network with desired channel thickness, which contribute significantly to occur an efficient exciton dissociation and migration in the photovoltaic devices. An additionally performed current measurements over the ternary film exhibit a profound increase in the mean current value (206 pA), which is almost twenty times more than the mean current value of binary P3HT:PCBM film. Further, an improved photon absorption in the NIR region (700-900 nm) clearly contributes to achieve a wide absorption property in the film. Thus, the added liquid crystalline material is found to be the main reason for the cause of major conformational changes, desired interpenetrating network with nanocrystallite formation as well as for the drastic improvement in charge carrier properties of P3HT:PCBM film.

Acknowledgements

This research was supported by the Solar Energy Research Initiative (Project code: DST/TMC/SERI/FR/201), Department of Science and Technology (DST), Govt. of India, New Delhi. The work of Ahipa T.N. was supported by the Jain University, through the postdoctoral fellowship and Anoop K.M. was supported by the Jain University, through the Ph.D. research fellowship. Special thanks to Bruker Center of Excellence, Sahakar Nagar, Bangalore for providing AFM facility.

References

- [1] H. Tsai, Z. Xu, R.K. Pai, L. Wang, A.M. Dattelbaum, A.P. Shreve, H.-L. Wang, M. Cotlet, *Chem. Mater.* 23 (2011) 759–761.
- [2] H. Zhou, L. Yang, W. You, *Macromolecules* 45 (2012) 607–632.
- [3] Z. He, C. Zhong, S. Su, M. Xu, H. Wu, Y. Cao, *Nat. Photon.* 6 (2012) 591–595.
- [4] J. You, L. Dou, K. Yoshimura, T. Kato, K. Ohya, T. Moriarty, K. Emery, C.-C. Chen, J. Gao, G. Li, Y. Yang, *Nat. Commun.* 4 (2013) 1446.
- [5] J.-Y. Lee, W.-S. Shin, J.-R. Haw, D.-K. Moon, *J. Mater. Chem.* 19 (2009) 4938–4945.
- [6] J.Y. Lee, S.W. Heo, H. Choi, Y.J. Kwon, J.R. Haw, D.K. Moon, *Sol. Energy Mater. Sol. Cells* 93 (2009) 1932–1938.
- [7] P.W.M. Blom, V.D. Mihailetschi, L.J.A. Koster, D.E. Markov, *Adv. Mater.* 19 (2007) 1551–1566.
- [8] Y. Wang, L. Yang, C. Yao, W. Qin, S. Yin, F. Zhang, *Sol. Energy Mater. Sol. Cells* 95 (2011) 1243–1247.
- [9] J.-M. Yun, J.-S. Yeo, J. Kim, H.-G. Jeong, D.-Y. Kim, Y.-J. Noh, S.-S. Kim, B.-C. Ku, S.-I. Na, *Adv. Mater.* 23 (2011) 4923–4928.
- [10] Y. Yao, J. Hou, Z. Xu, G. Li, Y. Yang, *Adv. Funct. Mater.* 18 (2008) 1783–1789.

- [11] B.A. Gregg, *MRS Bull.* 30 (2005) 20–22.
- [12] I.-W. Hwang, Q.-H. Xu, C. Soci, B. Chen, A.K.-Y. Jen, D. Moses, A.J. Heeger, *Adv. Funct. Mater.* 17 (2007) 563–568.
- [13] H. Ohkita, S. Cook, Y. Astuti, W. Duffy, S. Tierney, W. Zhang, M. Heeney, I. McCulloch, J. Nelson, D.D.C. Bradley, J.R. Durrant, *J. Am. Chem. Soc.* 130 (2008) 3030–3042.
- [14] K. Yao, Y. Chen, L. Chen, D. Zha, F. Li, J. Pei, Z. Liu, W. Tian, *J. Phys. Chem. C* 114 (2010) 18001–18011.
- [15] L. Yu, C. Li, Q. Li, F. Wang, J. Lin, J. Liu, S. Hu, H. Zheng and Z. a. Tan, *Org. Electron.* 23 (2015) 99-104.
- [16] F. Wang, Q. Xu, Z. a. Tan, L. Li, S. Li, X. Hou, G. Sun, X. Tu, J. Hou and Y. Li, *J. Mater. Chem. A* 2 (2014) 1318-1324.
- [17] X. Guo, C. Cui, M. Zhang, L. Huo, Y. Huang, J. Hou and Y. Li, *Energy Environ. Sci.* 5 (2012) 7943-7949.
- [18] S. J. Lou, J. M. Szarko, T. Xu, L. Yu, T. J. Marks and L. X. Chen, *J. Am. Chem. Soc.* 133 (2011) 20661-20663.
- [19] A. K. K. Kyaw, D. H. Wang, C. Luo, Y. Cao, T.-Q. Nguyen, G. C. Bazan and A. J. Heeger, *Adv. Energy Mater.* 4 (2014) 1301469.
- [20] D. K. Yang and S. T. Wu, *Fundamentals of Liquid Crystal Devices*, Wiley, New York, 2006.
- [21] D. Han, X. Tong, Y. Zhao, Y. Zhao, *Angew. Chem. Int. Ed.* 49 (2010) 9162–9165.
- [22] X. Tong, D. Han, D. Fortin, Y. Zhao, *Adv. Funct. Mater.* 23 (2013) 204–208.
- [23] L. Schmidt-Mende, A. Fechtenkötter, K. Müllen, E. Moons, R.H. Friend, J.D. MacKenzie, *Science* 293 (2001) 1119–1122.

- [24] Z. He, C. Zhong, X. Huang, W.-Y. Wong, H. Wu, L. Chen, S. Su, Y. Cao, *Adv. Mater.* 23 (2011) 4636–4643.
- [25] A. Iwan, A. Sikora, V. Hamplová, A. Bubnov, *Liq. Cryst.* (2015) 1–9. DOI: 10.1080/02678292.2015.1011243
- [26] A. Iwan, M. Palewicz, M. Krompiec, M. Grucela-Zajac, E. Schab-Balcerzak, A. Sikora, *Spectrochim. Acta A* 97 (2012) 546–555.
- [27] M. Palewicz, A. Iwan, M. Sibinski, A. Sikora, B. Mazurek, *Energy Procedia* 3 (2011) 84–91.
- [28] A. Iwan, E. Schab-Balcerzak, D. Pocięcha, M. Krompiec, M. Grucela, P. Bilski, M. Kłosowski, H. Janeczek, *Opt. Mater.* 34 (2011) 61–74.
- [29] W. Zhou, J. Shi, L. Lv, L. Chen, Y. Chen, *Phys. Chem. Chem. Phys.* 17 (2015) 387–397.
- [30] S. Jeong, Y. Kwon, B.-D. Choi, H. Ade and Y. S. Han, *Appl. Phys. Lett.* 96 (2010) 183305.
- [31] K. Yuan, L. Chen, Y. Chen, *J. Mater. Chem. C* 2 (2014) 3835–3845.
- [32] T.N. Ahipa, A.V. Adhikari, *Tetrahedron Lett.* 55 (2014) 495–500.
- [33] Y. Kim, S.A. Choulis, J. Nelson, D.D.C. Bradley, S. Cook, J.R. Durrant, *J. Mater. Sci.* 40 (2005) 1371–1376.
- [34] J.G.F. Hide, H. Wang, *Synth. Met.* 84 (1997) 979–980.
- [35] C.H. Lee, G. Yu, D. Moses, K. Pakbaz, C. Zhang, N.S. Sariciftci, A.J. Heeger, F. Wudl, *Phys. Rev. B* 48 (1993) 15425–15433.
- [36] L. Smilowitz, N.S. Sariciftci, R. Wu, C. Gettinger, A.J. Heeger, F. Wudl, *Phys. Rev. B* 47 (1993) 13835–13842.
- [37] P.J. Brown, D.S. Thomas, A. Köhler, J.S. Wilson, J.-S. Kim, C.M. Ramsdale, H. Sirringhaus, R.H. Friend, *Phys. Rev. B* 67 (2003) 064203.
- [38] F.C. Spano, *J. Chem. Phys.* 122 (2005) 234701.

- [39] U. Zhokhavets, T. Erb, G. Gobsch, M. Al-Ibrahim, O. Ambacher, *Chem. Phys. Lett.* 418 (2006) 347–350.
- [40] P. Peumans, S. Uchida, S.R. Forrest, *Nature* 425 (2003) 158–162.
- [41] W. Ma, C. Yang, X. Gong, K. Lee, A.J. Heeger, *Adv. Funct. Mater.* 15 (2005) 1617–1622.
- [42] L. Lu, T. Xu, W. Chen, J.M. Lee, Z. Luo, I.H. Jung, H.I. Park, S.O. Kim, L. Yu, *Nano Lett.* 13 (2013) 2365–2369.
- [43] J.Y. Oh, M. Shin, T.I. Lee, W.S. Jang, Y. Min, J.-M. Myoung, H.K. Baik, U. Jeong, *Macromolecules* 45 (2012) 7504–7513.
- [44] X. Yang, J. Loos, *Macromolecules* 40 (2007) 1353–1362.
- [45] M. Dante, J. Peet, T.-Q. Nguyen, *J. Phys. Chem. C* 112 (2008) 7241–7249.
- [46] D.T. Duong, H. Phan, D. Hanifi, P.S. Jo, T.-Q. Nguyen, A. Salleo, *Adv. Mater.* 26 (2014) 6069–6073.

Graphical Abstract:

Trihydrazone-functionalized cyanopyridine liquid crystal is introduced into the photoactive layer as processing additive to acquire improved interpenetrating network and charge carrier mobility.

